

**Keywords:**

stellar winds, mass loss, stellar evolution, supernovae

Author for correspondence:

Jorick S. Vink

e-mail: jsv@arm.ac.uk

Mass loss and stellar superwinds

Jorick S. Vink¹

¹Armagh Observatory, College Hill, Armagh BT61 9DG, Northern Ireland

Mass loss bridges the gap between massive stars and supernovae (SNe) in two major ways: (i) theoretically it is the amount of mass lost that determines the mass of the star prior to explosion, and (ii) observations of the circumstellar material around SNe may teach us the type of progenitor that made the SN. Here, I present the latest models and observations of mass loss from massive stars, both for canonical massive O stars, as well as very massive stars (VMS) that show Wolf-Rayet type features.

1. Introduction: massive stars with superwinds before explosion

The progenitor stars of Type IIP(lateau) Supernovae (SNe) have been established to be red supergiants (RSGs) (Van Dyk et al. 2002; Smartt et al. 2009), but the more massive progenitors of Type IIb, IIc, Ibn, Ibc have yet to be identified. Traditionally, SN progenitors have been pinpointed using photometry, but since recently a new method of rapid “flash” spectroscopy has become available: Gal-Yam et al. (2014) discovered a stellar wind in the SN spectrum of the Type IIb supernova 2013cu, which they attributed to be a Wolf-Rayet (WR) star due to the strong emission lines in its spectrum (see Fig. 1).

However, Groh (2014) and Gräfener & Vink (2016) modelled the spectrum, arguing the narrow lines from 2013cu are representative of a luminous blue variable (LBV) or other post-RSG object. Gräfener & Vink (2016) derived a huge mass loss prior to explosion, arguing the progenitor had been subjected to a *superwind*, due to its increasing radiation pressure and associated Eddington factor $\Gamma_e = g_{\text{rad}}/g_{\text{grav}} = \sigma_e L / (4\pi cGM)$ prior to explosion (see Fig. 2)

It is clear that we need to understand the mass-loss properties of massive stars at high Γ_e , but before addressing this aspect we first review the mass-loss rates of normal O-stars (at moderate Γ_e parameters). I assume basic knowledge of radiation-driven wind theory, but see Owocki (2015) and Vink (2015) for more information.

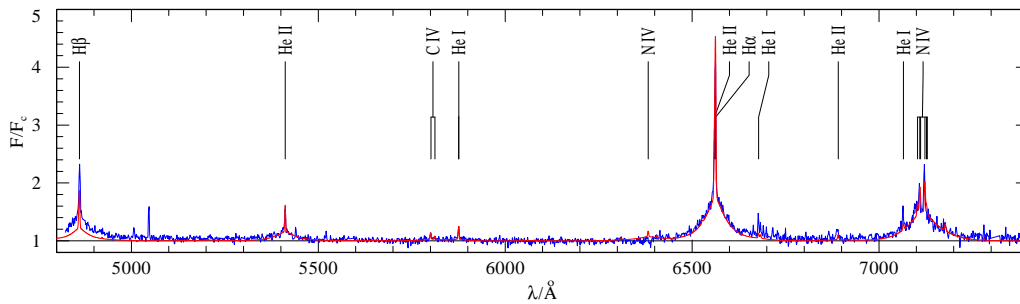


Figure 1. Model fit to the observed spectrum of the IIb supernova SN 2013cu, 15.5 hours after explosion (Gal-Yam et al. 2014). See Gräfenner & Vink (2016) for more details on the model fit.

2. Normal O star wind models

The radiation-driven wind theory was developed in the 1970s by Lucy & Solomon (1970) and Castor, Abbott & Klein (1975; hereafter CAK). For many years it was thought that the strong, optically thick, lines of carbon, oxygen and nitrogen (CNO) were the most important wind drivers – due to the relatively high abundance of these elements – causing their presence in the ultraviolet (UV) spectra of early-type stars.

However, we now know that despite its relatively minor cosmic abundance, it is the millions of weak (and optically thin) iron (Fe) lines below the critical (sonic) point that set the mass-loss rates in massive O-star winds (Vink et al. 1999, 2000, 2001). The mass-loss recipes from these authors are now widely used in the evolution of massive stars, but questions have been raised regarding the absolute strengths of the normal¹ O-star winds, due to the widespread presence of wind inhomogeneities, or clumping (e.g. Puls et al. 2008; Cantiello et al. 2009).

3. Normal O star wind observations

Fullerton et al. (2006) highlighted the problem of wind clumping in the form of the so-called Phosphorus ν problem: if the winds of massive stars are inhomogeneous and the clumps can be treated in the micro-clumping approximation (see also Bouret et al. 2003), then the most likely solution for the P ν problem in the UV part of the spectrum would be *far* lower mass-loss rates (see Fig. 3), perhaps by an order-of-magnitude.

The P ν problem was solved when Oskinova et al. (2007) (see also Sundqvist et al. 2010; Surlan et al. 2013) introduced the concept of porosity or “macro-clumping”, previously constructed for X-ray observations, to the UV part of the spectrum (see Fig. 3). The P ν line can now be fit, without needing to reduce the empirical mass-loss rate excessively. The unclumped empirical mass-loss rates are still overestimated by a factor of the square-root of the clumping factor, but as long as clumping is moderate, with clumping factors 6-8, the reduced mass-loss rates (by factor 2-3) agree with the theoretical rates of Vink et al. (see the discussions in Repolust et al. 2004; Mokiej et al. 2007; Ramirez-Agudelo et al. 2016).

¹Furthermore, at low luminosities, with $\log(L/L_{\odot}) < 5.2$ there is a *weak wind* problem (Martins et al. 2005, Puls et al. 2008). This corresponds to spectral types later than O6.5V (Muijres et al. 2012) and may be due to a lack of subsonic radiative driving due to a recombination of Fe ν to IV at that T_{eff} . If true, this would imply the physics of an “inverse” bi-stability jump

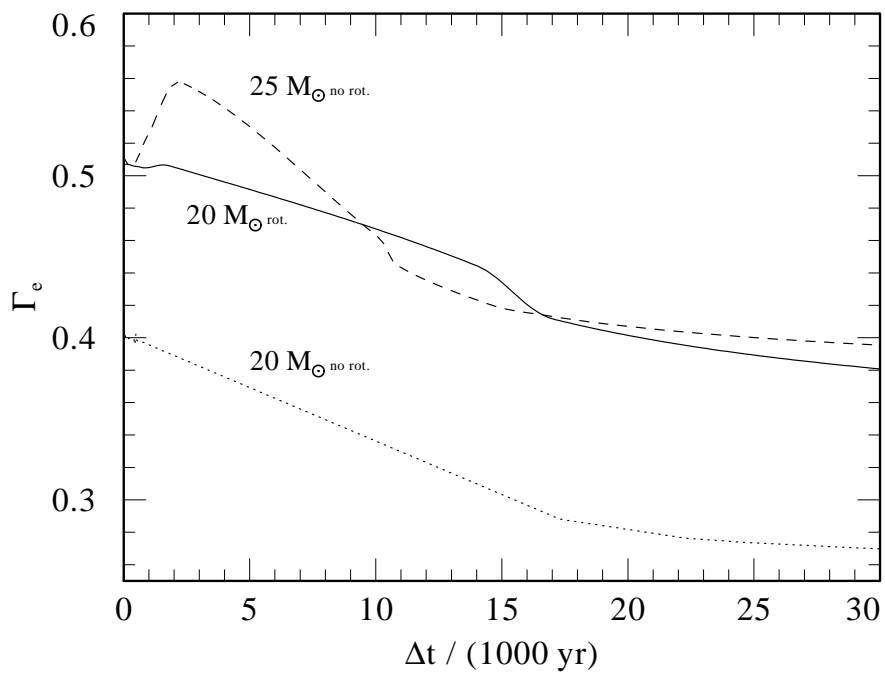


Figure 2. Eddington factor in the final thousands of years before expiration. See Gräfener & Vink (2016) with evolutionary model data from Ekström et al. (2012).

4. The first mass-loss calibration

For normal O-type stars, say in the luminosity range $\log(L/L_{\odot}) = 5.2 - 5.8$, there is no guarantee that the clumping factor is a factor 6-8, as may seemingly have been suggested in the previous paragraph. If the *true* clumping factor is larger than 6-8, the Vink et al. rates would be too large

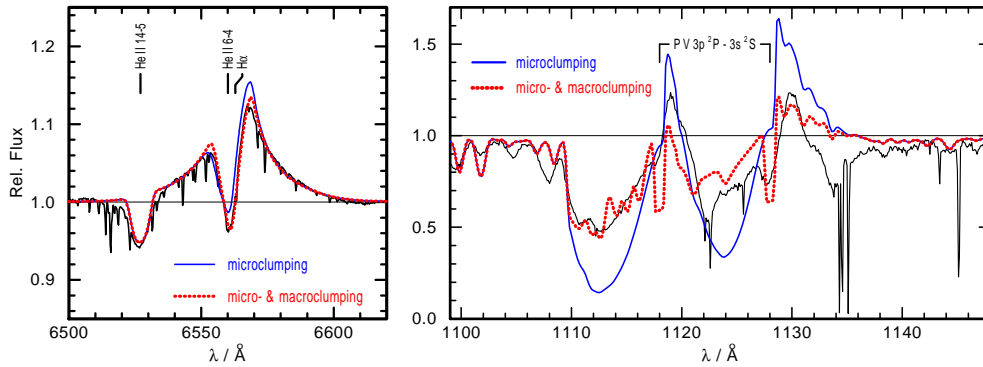


Figure 3. The phosphorus V problem, as solved by Oskinova et al. (2007) using optically thick “macro” clumps. The figure on the right is the ultraviolet P V spectrum of the O supergiant ζ Pup, whilst the figure on the left concerns the $H\alpha$ profile.

compared to empirical values. The interesting question is now if we can establish what the correct clumping factor is in O-star winds?

For the more extreme winds of Wolf-Rayet stars (including both classical WR stars, as well as very massive stars (VMS) of the WNh sequence) the spectral lines are in emission, and owing to the presence of electron scattering wings, which depend linearly on density (versus the quadratic density behaviour of the central recombination part of the emission line), one may constrain the clumping factor (Hillier et al. 1991). On the basis of this methodology the Potsdam group (e.g. Hamann & Koesterke 1998) usually quote clumping factors in the range 4–16, with mass-loss rate reductions for WR stars (in comparison to unclumped empirical rates) of $\sim 2 - 4$, with a reasonable average clumping factor of ~ 10 , i.e. a mass-loss rate reduction of ~ 3 (Hamann et al. 2008).

For decades it was known that Wolf-Rayet stars are special in comparison to O stars in that the wind efficiency number $\eta = \dot{M}v_\infty/(L/c)$ exceeds unity due to highly efficient multiple scattering (e.g. Gayley et al. 1995). However, it was not until it became clear that VMS with masses exceeding $150M_\odot$ exist (Crowther et al. 2010, Bestenlehner et al. 2011, Vink et al. 2015) that we were able to construct a mass (and luminosity) sequence of O and VMS-WNh stars, sampling the entire upper initial mass function (IMF), including the entire O-Of-Of/WN-WNh spectral sequence – and to utilize this to calibrate stellar wind mass-loss rates using the $\eta = \tau = 1$ relation (Vink & Gräfener 2012).

Vink & Gräfener (2012) showed that the transition luminosity between optically thin Of stars (with $\tau < 1$) and optically thick (with $\tau > 1$) WNh stars in the Arches cluster (based on CMFGEN modelling by Martins et al. 2008) could be utilised to derive the transition mass-loss rate. As this model-independent transition mass-loss rate agrees well with both the theoretical mass-loss rates of Vink et al., as well as the empirical mass-loss rates of Martins et al. (for an assumed

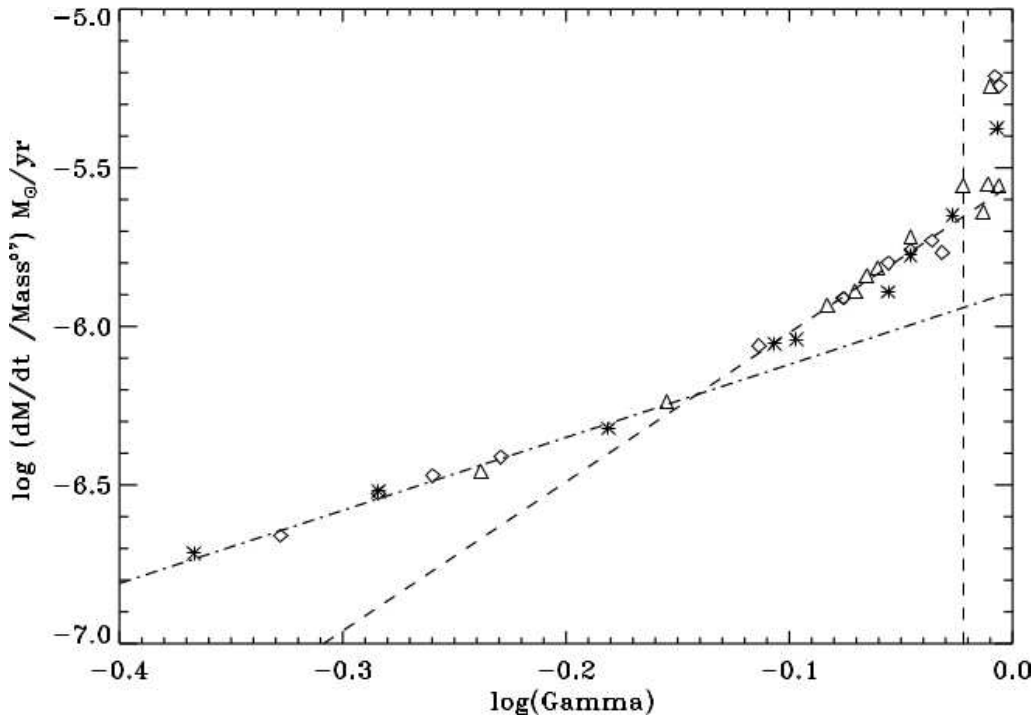


Figure 4. VMS mass-loss rates versus the Eddington factor, as predicted by Monte Carlo models of Vink et al. (2011) using a new parametrisation of the line acceleration by Müller & Vink (2008).

clumping factor of 10) this provides a strong consistency argument – resulting in the first mass-loss calibration in astronomy.

Moreover, this provides evidence for strong mass-loss for VMS, ensuring “evaporation” of Galactic stars due to mass loss. This would make it highly unlikely that exotic phenomena involving gamma-ray bursts (Vink & de Koter 2005), pair-instability SNe (Langer et al. 2007), or other super-luminous SNe (Quimby et al. 2011; Neill et al. 2011; Stoll et al. 2011; Lunnan et al. 2015; Leloudas et al. 2015; Vreeswijk et al. 2015; Chen et al. 2016) would take place at Galactic “high” metal content, but that low metallicity may be a prerequisite.

Moreover, the very existence of relatively massive stellar black holes, with masses $> 30M_{\odot}$ as recently discovered through gravitational waves (Abbott et al. 2016) would call for low-metallicity environments according to our wind models (Belczynski et al. 2010) – providing a relationship between the maximum mass of stellar black holes and metallicity.

5. Very Massive Stars with high Eddington factor

The previous section concluded that we know the mass-loss rates of massive stars at the transition luminosity very accurately. As long as the clumping factor for lower luminosity “normal” O-stars in the luminosity range $\log(L/L_{\odot}) = 5.2 - 5.8$ is not much larger than ~ 10 , we can be confident that the Vink et al. (2000) relation provides accurate mass-loss rates, as these rates have now been calibrated at the high mass-luminosity end, against a model independent anchor (which is clumping and porosity independent).

However, for VMS with luminosities *above* the transition luminosity, the Vink et al. relationship would *underestimate* the true mass-loss rates, as the Vink et al. (2000) relation was derived for optically thin winds, whilst VMS have winds that are optically thick (see also Gräfener & Hamann 2008; Gräfener et al. 2011).

In order to study the transition from optically thin to optically thick winds, Vink et al. (2011) computed Monte Carlo radiative acceleration models (based on an original concept by Abbott & Lucy 1985) into the regime of VMS up to $300M_{\odot}$. The results are shown in Fig. 4. The plot shows a relatively shallow slope for optically thin O-star winds with $\dot{M} \propto \Gamma^2$ (in reasonable agreement with CAK theory) at relatively low Γ values, turning into a much steeper slope, above the transition mass-loss rate, where $\dot{M} \propto \Gamma^5$ (see also Vink 2006). This steeper slope is not yet adopted into most stellar evolutionary models for VMS (e.g. Yusof et al. 2013; Koehler et al. 2015), although Chen et al. (2015) have made first attempts in this direction.

Figure 4 involves a set of theoretical computations for mass-loss rates at high Eddington factor Γ , relevant for VMS, but they have yet to be tested against observations. In order to test the transition from optically thin to optically thick winds, it is important to sample the upper IMF, which is only possible for the most massive clusters in the Local Universe. In the context of the VLT-Flames Tarantula Survey (VFTS; Evans et al. 2011), we have analyzed an unprecedentedly large sample (of 62) of the most massive Of-Of/WN- WNh stars in the 30 Doradus region of the Large Magellanic Cloud (LMC) using CMFGEN. The results are presented in Fig. 5 and in Bestenlehner et al. (2014). The most notable aspect of our empirical work is that we do indeed *confirm* the presence of a kink at a critical Γ value. Furthermore, the slope in the mass-loss relation of the upper Γ range was found to be 5, also in perfect agreement with our theoretical Monte Carlo models (Vink 2006; Vink et al. 2011).

It should be noted that this steep increase of \dot{M} above a critical Γ value cannot be explained by CAK theory, where the steep increase only takes place at Γ values extremely close to 1, unless one were to chance the CAK-parameter α at the kink, but to all intents and purposes, a change in α at the kink versus a kink in its own right, represent a similar physical effect, due to the increased optical depth.

Finally, we should note that despite the qualitative success regarding (i) the presence of a kink, and (ii) the value of the steep slope (of 5) at the high Γ end, the location of the kink in terms of the exact Γ value (and related to different opacity treatments, and derivations of the Γ factor for (in)homogeneous stellar evolution models) implies that there is still quantitative work ahead of us in establishing accurate empirical and theoretical mass-loss rates for VMS.

A similar uncertainty exists for massive stars in evolved evolutionary phases, e.g. in the LBV and classical WR phase, where the Γ factor might be substantial too.

6. LBVs: Envelope Inflation and Bi-stability Jumps

Luminous Blue Variables (or LBVs) are objects that change spectral type (from early B to late A/early F) on timescales of years to decades (Humphreys & Davidson 1994; Fig. 6). This physical phenomenon with associated ΔV of $\sim 1 - 2$ magnitudes is usually referred to as the ‘‘S Dor’’ cycle². The reason for the apparent changes in effective temperature has not been fully understood, but the leading contender is thought to be envelope inflation (Gräfener et al. 2012, Vink 2012; Sanyal et al. 2015). The typical structure of a massive star that is subject to envelope inflation is depicted in Fig. 7. This core-halo structure (Ishii et al. 1999; Petrovic et al. 2005; Yungelson et al. 2008; Gräfener et al. 2012) includes a very low density envelope beneath a thin shell (associated with the density inversion in Fig. 7).

Whilst models including the OPAL (Iglesias & Rogers 1996) opacities showed the presence of an inflated envelope in stellar structure and evolution calculations, it was not until Gräfener et al. (2012) presented an in-depth analysis of envelope inflation around the Fe opacity peak, that an analytic formula for radius extension was derived:

$$\frac{R_{\text{out}}}{R_{\text{in}}} = \frac{1}{1 - W} \quad W = \frac{\Delta P_{\text{rad}} R_{\text{in}}}{GM \rho_{\text{mean}}} \quad (6.1)$$

The formula indicates that envelope extension can be understood in terms of the width of the Fe opacity peak in terms of ΔP_{rad} divided by potential energy of the envelope (see Fig. 8).

²In contrast to the giant eruption LBVs like P Cygni and η Car where $\Delta V = 5$, or more

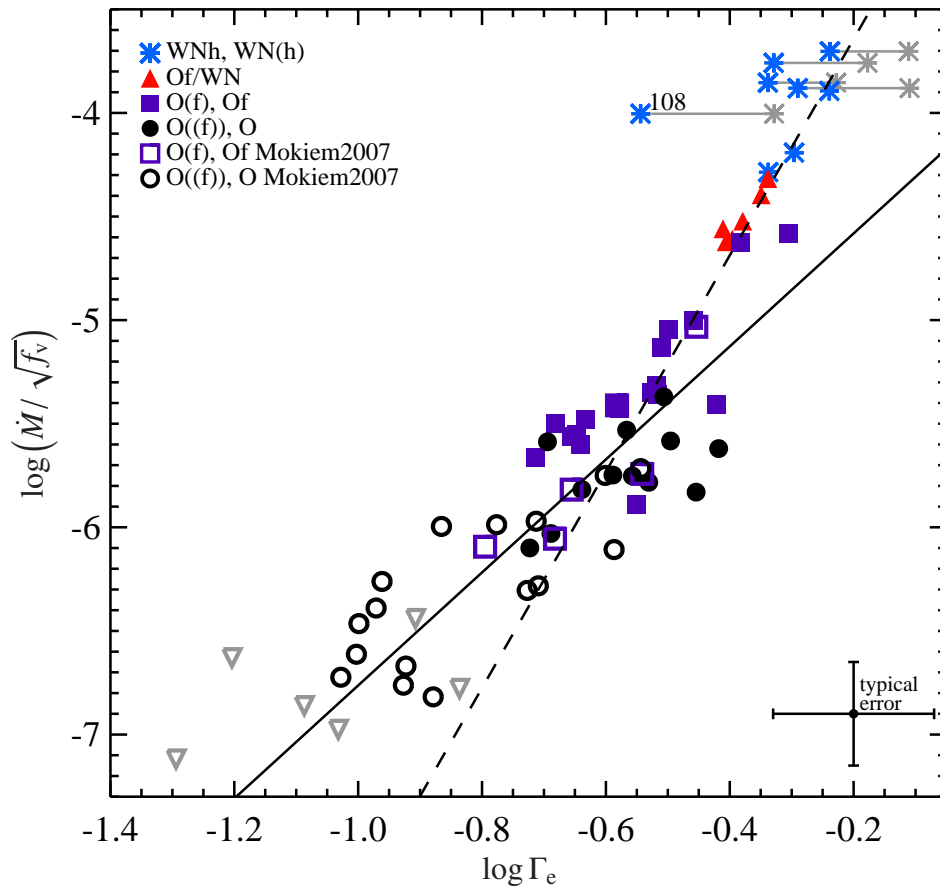


Figure 5. Unclumped $\log \dot{M}$ (divided by the inverse of the square-root of the clumping factor) versus $\log \Gamma_e$ from Bestenlehner et al. (2014). Solid line: $\dot{M} - \Gamma$ relation for O stars. The different symbols indicate stellar sub-classes. Dashed line: the steeper slope of the Of/WN and WNH stars. The *kink* occurs at $\log \Gamma_e = -0.58$. The grey asterisks indicate the position of the stars with $Y > 0.75$ under the assumption of core He-burning. The grey upside down triangles are stars from Mokiem et al. (2007) which have only an upper limit in \dot{M} and are excluded from the fit.

If and when an LBV inflates its envelope, presumably due to its approach of the Eddington limit, it is expected to cross the upper Hertzsprung-Russell diagram (HRD), thereby encountering certain discontinuities in mass-loss rates at the first (21 000; Pauldrach & Puls 1990; Lamers et al. 1995; Vink et al. 1999; Petrov et al. 2016) and second (10 000K; Lamers et al. 1995; Vink et al. 1999; Petrov et al. 2016) bi-stability jumps, which are due to the recombination of Fe IV to III at the first jump, and Fe III to Fe II at the second jump.

The first bi-stability jump was indicated in the HRD of Fig. 6 and has been relatively well-studied. The second bi-stability jump was only recently studied in detail (using CMFGEN models) and the results are shown in Fig. 9. As LBVs have recently been suggested to be the direct progenitors of the transitional supernova types IIb and IIc (arrow line) (Kotak & Vink 2006; Smith 2015), with enhanced mass loss prior to explosion, there has been renewed interest in the physical mechanism for this mass loss. To investigate the physical ingredients that may play a role in the radiative acceleration of LBVs, Petrov et al. calculated blue supergiant wind models with the CMFGEN non-LTE model atmosphere code over an effective temperature range between 30000 and 8800 K, studying and confirming the existence of both the first and second bi-stability jumps of Vink et al. (1999). However, Petrov et al. (2016) found them to occur at somewhat lower

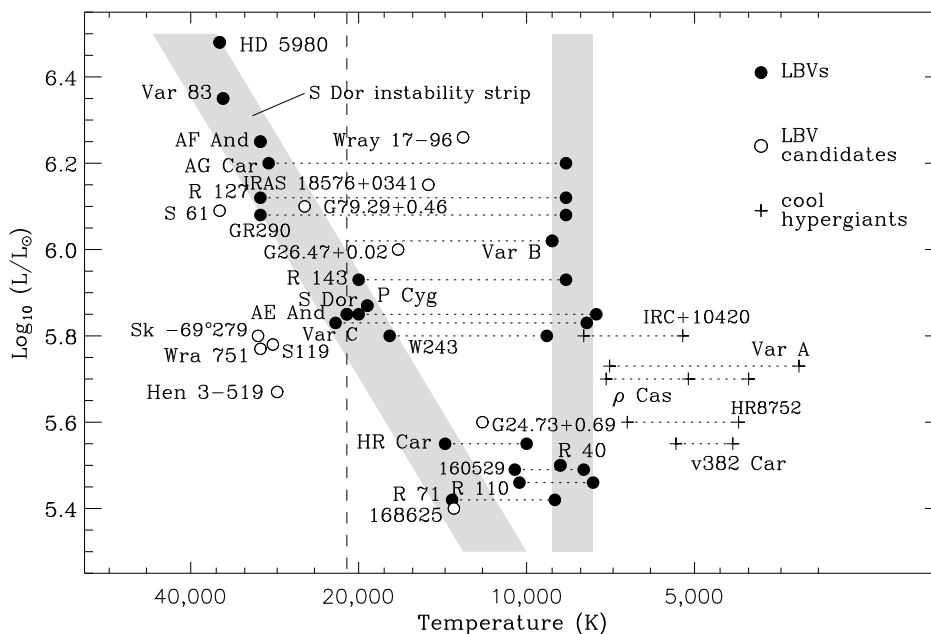


Figure 6. The location of the LBVs (black circles) and candidates (open circles) in the Hertzsprung-Russell diagram. The cool yellow hypergiants are indicated with pluses. The slanted and vertical grey bands represent visual minimum and maximum respectively. The dashed vertical line at 21 000K indicates the location of first the bi-stability jump. The figure has been adapted from Humphreys & Davidson (1994); Smith et al. (2004); and Vink (2012).

T_{eff} (20 000 and 9 000 K), in better accord with the observed locations (Lamers et al. 1995), which would imply that stars may evolve towards lower T_{eff} before strong mass-loss is induced by the bi-stability jumps.

When the combined effects of the second bi-stability jump and the proximity to Eddington limit are accounted for, Petrov et al. found a dramatic increase in the mass-loss rate by up to a factor of 30 (see Fig. 9), which may have consequences for the evolution of massive stars prior to expiration, as can be gleaned from Fig. 2.

Further investigation of both bi-stability jumps is expected to lead to a better understanding of discrepancies between empirical modelling and theoretical mass-loss rates reported in the literature, and to provide key inputs for the evolution of both normal AB supergiants and LBVs, as well as their subsequent supernova type II explosions.

7. Conclusion

Stellar (super)winds are not only important for correctly predicting the forwards evolution of massive stars from the zero-age main-sequence (ZAMS) towards explosion, but also for the *backwards* identification of SN progenitors. For both aspects it is crucial to understand that radiation-driven wind models do not only depend on stellar luminosity (and metallicity), but also on effective temperature (especially at bi-stability jumps) and stellar mass (and/or the Eddington factor Γ).

Only when we are able to correctly predict the mass-loss rates of evolved massive stars (at high Γ) as a function of all these stellar parameters will we be able to correctly model the evolution & fate and atmospheres of massive stars, including their ionizing radiation as a function of metallicity – and cosmic time.

Acknowledgements. Insert acknowledgment text here.

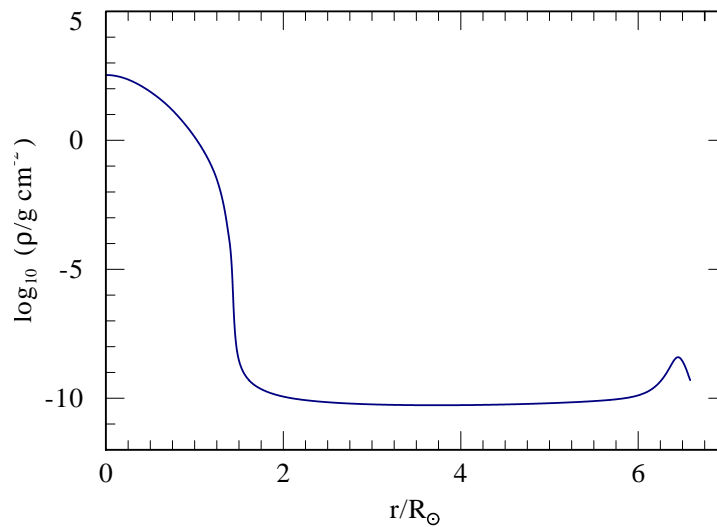


Figure 7. The peculiar density structure of a massive star with an inflated envelope. The model has a very extended low-density envelope over many stellar radii (Gräfener et al. 2012).

References

- Abbott, D. C., & Lucy, L. B. 1985, *ApJ* 288, 679
 Abbott, B. P., Abbott, R., Abbott, T. D., et al. 2016, *ApJL* 818, 22
 Belczynski, K., Bulik, T., Fryer, C. L., et al. 2010, *ApJ* 714, 1217
 Bestenlehner, J. M., Vink, J. S., Gräfener, G., et al. 2011, *A&A* 530, L14
 Bestenlehner, J. M., Gräfener, G., Vink, J. S., et al. 2014, *A&A* 570, A38
 Bouret, J.-C., Lanz, T., Hillier, D. J., et al. 2003, *ApJ* 595, 1182
 Cantiello, M., Langer, N., Brott, I., et al. 2009, *A&A* 499, 279
 Castor, J. I., Abbott, D. C., & Klein, R. I. 1975, *ApJ* 195, 157
 Chen, T.-W., Smartt, S. J., Yates, R. M., et al. 2016, arXiv:1605.04925
 Chen, Y., Bressan, A., Girardi, L., et al. 2015, *MNRAS* 452, 1068
 Crowther, P. A., Schnurr, O., Hirschi, R., et al. 2010, *MNRAS* 408, 731
 Ekström, S., Georgy, C., Eggenberger, P., et al. 2012, *A&A* 537, A146
 Evans, C. J., Taylor, W. D., Hénault-Brunet, V., et al. 2011, *A&A* 530, A108
 Fullerton, A. W., Massa, D. L., & Prinja, R. K. 2006, *ApJ* 637, 1025
 Gal-Yam, A., Arcavi, I., Ofek, E. O., et al. 2014, *Nature* 509, 471
 Gayley, K. G., Owocki, S. P., & Cranmer, S. R. 1995, *ApJ* 442, 296

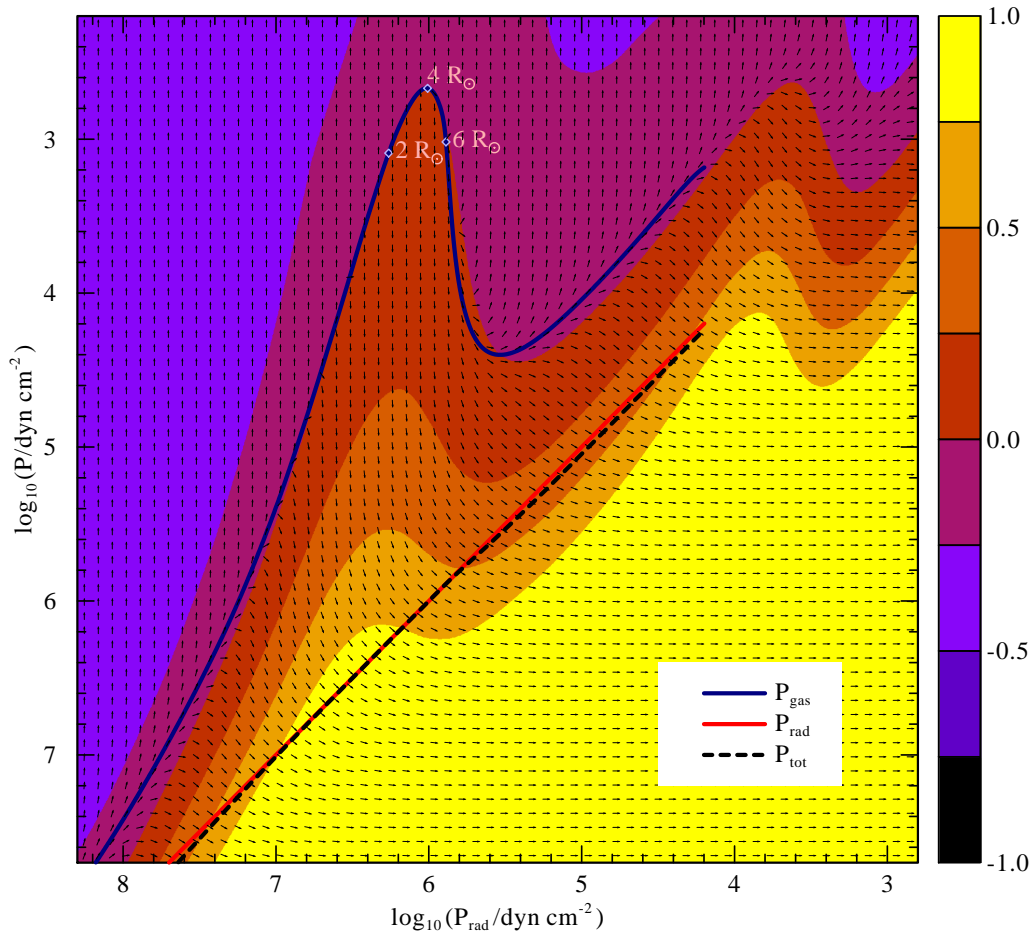


Figure 8. Envelope solution in the $P_{\text{rad}}-P_{\text{gas}}$ plane. The colours indicate the logarithm of the Eddington factor Γ , for given P_{rad} and P_{gas} , according to the OPAL opacity tables – for a pure He model with $23 M_{\odot}$ (Gräfener et al. 2012). The envelope solution almost precisely follows a path with $\Gamma = 1$. The radii of 2, 4, and $6 R_{\odot}$ within the inflated envelope are indicated. The arrows indicate the slope of the solution.

- Gräfener, G., & Hamann, W.-R. 2008, A&A 482, 945
 Gräfener, G., & Vink, J. S. 2016, MNRAS 455, 112
 Gräfener, G., Vink, J. S., de Koter, A., & Langer, N. 2011, A&A 535, A56
 Gräfener, G., Owocki, S. P., & Vink, J. S. 2012, A&A 538, A40
 Groh, J. H. 2014, A&A 572, L11
 Hamann, W.-R., & Koesterke, L. 1998, A&A 335, 1003
 Hamann, W.-R., Feldmeier, A., & Oskinova, L. M. 2008, Clumping in Hot-Star Winds
 Hillier, D. J. 1991, A&A 247, 455
 Hillier, D. J., & Miller, D. L. 1998, ApJ 496, 407
 Humphreys, R. M., & Davidson, K. 1994, PASP 106, 1025
 Iglesias, C. A., & Rogers, F. J. 1996, ApJ 464, 943
 Ishii, M., Ueno, M., & Kato, M. 1999, PASJ 51, 417
 Köhler, K., Langer, N., de Koter, A., et al. 2015, A&A 573, A71
 Kotak, R., & Vink, J. S. 2006, A&A 460, L5
 Lamers, H. J. G. L. M., Snow, T. P., & Lindholm, D. M. 1995, ApJ 455, 269
 Langer, N., Norman, C. A., de Koter, A., et al. 2007, A&A 475, L19
 Leloudas, G., Schulze, S., Krühler, T., et al. 2015, MNRAS 449, 917
 Lucy, L. B., & Solomon, P. M. 1970, ApJ 159, 879

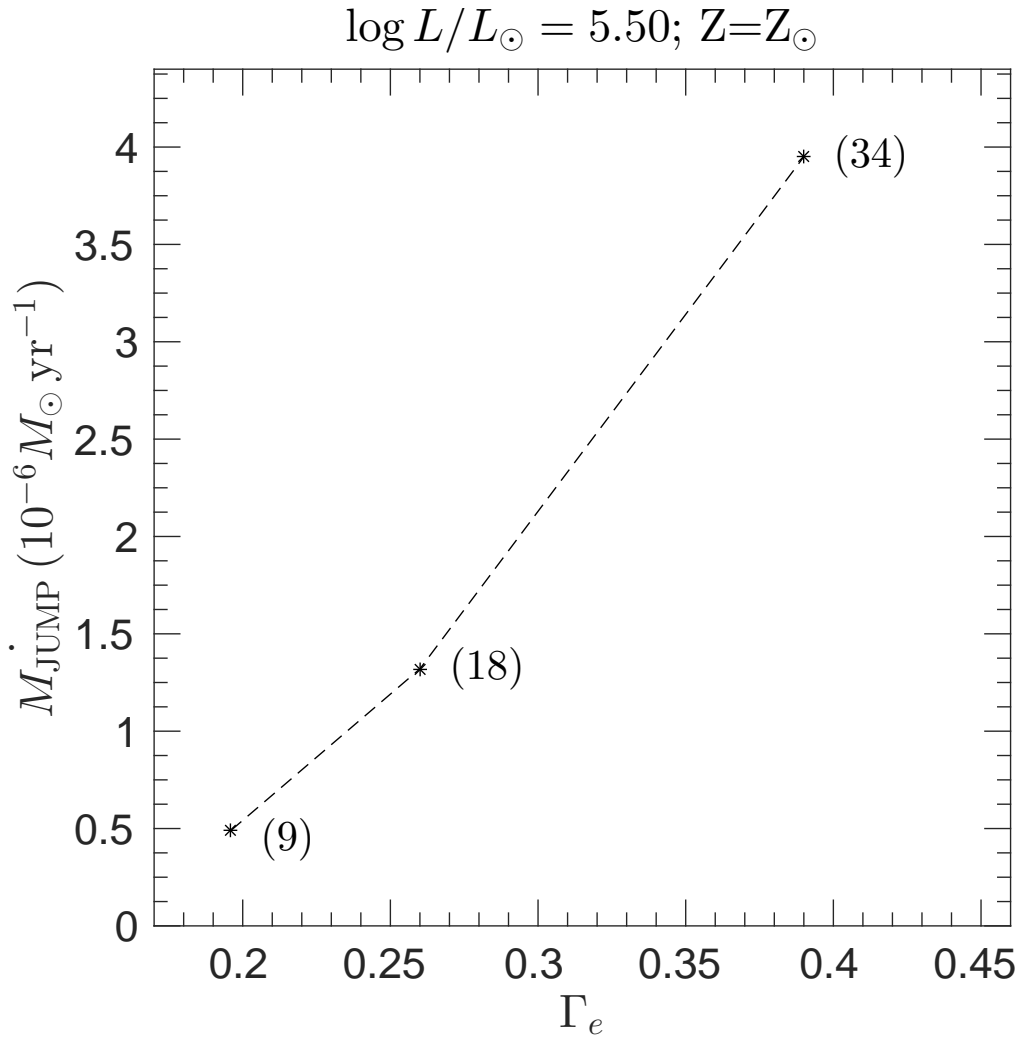


Figure 9. Theoretical mass-loss models for mass-loss rates at the *second* bi-stability jump, as computed with the CMFGEN (Hillier & Miller 1998) code by Petrov et al. (2016).

- Lunnan, R., Chornock, R., Berger, E., et al. 2014, ApJ 787, 138
 Martins, F., Schaerer, D., Hillier, D. J., et al. 2005, A&A 441, 735
 Martins, F., Hillier, D. J., Paumard, T., et al. 2008, A&A 478, 219
 Mokiem, M. R., de Koter, A., Vink, J. S., et al. 2007, A&A 473, 603
 Muijres, L. E., Vink, J. S., de Koter, A., Müller, P. E., & Langer, N. 2012, A&A 537, A37
 Müller, P. E., & Vink, J. S. 2008, A&A 492, 493
 Neill, J. D., Sullivan, M., Gal-Yam, A., et al. 2011, ApJ 727, 15
 Oskinova, L. M., Hamann, W.-R., & Feldmeier, A. 2007, A&A 476, 1331
 Owocki, S. P. 2015, Very Massive Stars in the Local Universe, 412, 113
 Pauldrach, A. W. A., & Puls, J. 1990, A&A 237, 409
 Petrov, B., Vink, J. S., & Gräfener, G. 2016, MNRAS 458, 1999
 Petrovic, J., Pols, O., & Langer, N. 2006, A&A 450, 219
 Puls, J., Vink, J. S., & Najarro, F. 2008, ARAA 16, 209
 Quimby, R. M., Kulkarni, S. R., Kasliwal, M. M., et al. 2011, Nature 474, 487
 Sanyal, D., Grassitelli, L., Langer, N., & Bestenlehner, J. M. 2015, A&A 580, A20
 Smartt, S. J., Eldridge, J. J., Crockett, R. M., & Maund, J. R. 2009, MNRAS 395, 1409
 Smith, N. 2015, Very Massive Stars in the Local Universe, 412, 227

- Smith, N., Vink, J. S., & de Koter, A. 2004, *ApJ* 615, 475
- Stoll, R., Prieto, J. L., Stanek, K. Z., et al. 2011, *ApJ* 730, 34
- Sundqvist, J. O., Puls, J., & Feldmeier, A. 2010, *A&A* 510, A11
- Šurlan, B., Hamann, W.-R., Aret, A., et al. 2013, *A&A* 559, A130
- Van Dyk, S. D., Garnavich, P. M., Filippenko, A. V., et al. 2002, *PASP* 114, 1322
- Vink, J. S. 2006, *Stellar Evolution at Low Metallicity: Mass Loss, Explosions, Cosmology*, 353, 113
- Vink, J. S. 2012, *Eta Carinae and the Supernova Impostors*, 384, 221
- Vink, J. S. 2015, *Very Massive Stars in the Local Universe*, 412, 77
- Vink, J. S., & de Koter, A. 2005, *A&A* 442, 587
- Vink, J. S., & Gräfener, G. 2012, *ApJL* 751, L34
- Vink, J. S., de Koter, A., & Lamers, H. J. G. L. M. 1999, *A&A* 350, 181
- Vink, J. S., de Koter, A., & Lamers, H. J. G. L. M. 2000, *A&A* 362, 295
- Vink, J. S., de Koter, A., & Lamers, H. J. G. L. M. 2001, *A&A* 369, 574
- Vink, J. S., Muijres, L. E., Anthonisse, B., et al. 2011, *A&A* 531, A132
- Vink, J. S., Heger, A., Krumholz, M. R., et al. 2015, *Highlights of Astronomy*, 16, 51
- Vreeswijk, P. M., Savaglio, S., Gal-Yam, A., et al. 2014, *ApJ* 797, 24
- Yungelson, L. R., van den Heuvel, E. P. J., Vink, J. S., Portegies Zwart, S. F., & de Koter, A. 2008, *A&A* 477, 223
- Yusof, N., Hirschi, R., Meynet, G., et al. 2013, *MNRAS* 433, 1114